Real-Time Epileptic Seizure Detection During Sleep Using Passive Infrared Sensors

Ouday Hanosh, Rashid Ansari, *Fellow, IEEE*, Khaled Younis, and A. Enis Cetin, *Fellow, IEEE*

***Abstract*— This paper addresses the problem of detecting epileptic seizures experienced by a human subject during sleep. Commonly used solutions to this problem mostly rely on detecting motion due to seizures using contact-based sensors or video-based sensors. We seek a low-cost, low-power alternative that can sense motion without making direct contact with the subject and provides high detection accuracy. We investigate the use of Passive InfraRed (PIR) sensors to sense human body motion caused by epileptic seizures during sleep which makes the body shake and causes the PIR sensor to generate an oscillatory output signal. This signal can be distinguished from that of ordinary motions during sleep using analysis with machine learning algorithms. The supervised hidden Markov model algorithm (HMM) and a 1-D and 2-D convolutional neural network (ConvNet) are used to classify the data set of the PIR sensor output into the occurrence of epileptic seizures, ordinary motions, or absence of motion. The method was tested on the PIR signals captured at 1 m from 33 recruited healthy subjects who, after watching seizure videos, either moved their body on a bed to simulate a seizure, ordinary motion, or lay still. The HMM algorithm attained 97.03% accuracy, while 1D-ConvNet and 2D-ConvNet attained an accuracy of 96.97% and 98.98%, respectively. All simulated seizures were successfully detected, with errors occurring only in distinguishing between ordinary motion and no motion, thereby demonstrating the potential for using PIR sensors in the epileptic seizure detection.**

***Index Terms*— PIR sensor, epileptic seizure, hidden Markov model (HMM), ConvNet, max-pooling, sensing unit (SU).**

I. Introduction

THE World Health Organization (WHO) has reported that approximately 50 million people world-wide suffer from a chronic non-communicable disorder of the brain, which is known as epilepsy. During an epileptic seizure, the brain cannot respond to normal activities. Many technologies and methods are being developed to detect occurrence of epileptic seizures in a human suffering from epilepsy [1]–[14]. Most of the technologies are based on sensors that can detect body movements and/or heartbeat, such as pulse oxymetry and micro-electromechanical sensors [1]. These sensors are small and may be attached to a human body, but such wearable sensors may bother a patient during sleep or patients may forget to wear them. Usually, these sensors need a wireless communication channel to transmit the signal for processing.

Another way to detect the epileptic seizure is to measure the brain electrical activity with electrocardiography (ECG) [2]. Although ECG provides reliable data to detect epileptic seizures, it is very difficult for a patient to wear the ECG electrodes during sleep and for a long period.

Systems based on accelerometer devices are also used to detect a type of seizure known as motor seizure, which is different from ordinary body motion during sleep [3], [5]. Video monitoring and night-vision camera systems are also used to detect epileptic seizures by tracking the path of moving objects (patient's limbs and other body parts) over time [8]. In addition to the high cost of such cameras, patients may feel uncomfortable with such monitoring during sleep due to privacy concerns. Another type of system uses a mattress sensor to detect the motor activity of the patient during sleep. The seizure detection accuracy of this system is 80% [9].

Our proposed method is based on passively detecting the infrared emissions from the human body during sleep. A non-medical Passive InfraRed (PIR) sensor is used to collect the infrared signal and detect body movements. The distance between a sleeping patient and the PIR sensor is typically 1 meter up to 11 meters when equipped with a wide-angle lens to increase the area of detection. Different machine learning algorithms were devised and investigated for classifying the types of body motion during sleep to indicate the occurrence or non-occurrence of seizures. The rest of the paper is organized as follows. Section II demonstrates the relation between epileptic seizures and sleep stages. Section III presents the proposed method. Classification and feature extraction using deep learning networks are explained in Section IV. The performance metrics of the classification methods are described in Section V. Section VI discusses the performance results of the proposed method. Finally, the conclusion of this study is provided in Section VII.

II. The Relationship Between Epileptic Seizures and Sleep Stages

According to many studies, the relationship between sleep and epilepsy has been known since the ancient Greek times [25]–[27]. This relationship is based on two major factors: the epilepsy syndrome and the stage of sleep. Sleep is

Manuscript received February 8, 2019; accepted March 14, 2019. Date of publication March 26, 2019; date of current version July 3, 2019. The work of A. E. Cetin was supported in part by NSF under Grant 1739396. The associate editor coordinating the review of this paper and approving it for publication was Dr. Shanhong Xia. *(Corresponding author: Ouday Hanosh.)*

O. Hanosh and R. Ansari are with the Electrical and Computer Engineering Department, University of Illinois at Chicago (UIC), Chicago, IL 60607 USA (e-mail: ohanos2@uic.edu; ransari@uic.edu).

K. Younis is with the Computer Engineering Department, School of Engineering, The University of Jordan, Amman 11942, Jordan (e-mail: younis@ju.edu.jo).

A. E. Cetin is with the Electrical and Computer Engineering Department, University of Illinois at Chicago (UIC), Chicago, IL 60607 USA, on leave from Bilkent University, Ankara, Turkey (e-mail: aecyy@uic.edu).

Digital Object Identifier 10.1109/JSEN.2019.2907664

broadly divided into three stages-wake, Non-Rapid Eye Movement (NREM) stage and Rapid Eye Movement (REM) stage. NREM sleep has been linked to strengthening of the connection between brain cells while the REM stage has been linked to dreams. According to the American Academy of Sleep Medicine (AASM), the NREM stage may be divided into three stages. The first two stages are known as light sleep while the third stage is known as deep sleep, or Slow-Wave Sleep (SWS) [28]. Stage one of the NREM sleep lasts for approximately 10 minutes during which muscles are relaxed, whereas, in stage two, breathing and the heart rate are observed to slow down. This stage lasts around 20 minutes and it has been observed that patients with epilepsy experience seizures during this sleep stage and are characterized by sudden and unusual movements of arms and legs, screams, and jerky movements. Such seizures may lead to injuries, including concussions, broken bones, or even Sudden Unexpected Death in Epilepsy (SUDEP) if the patients are not attended to in a timely manner [25], [26], [28]. It is therefore important to reliably detect the occurrence of seizures during sleep. This motivated our search for affordable, low-power, contact-free solutions to this problem. This led us to the investigation of PIR sensors for epilepsy detection based on our prior knowledge of the effectiveness of PIR sensors in motion detection applications. Detection of an epileptic seizure during sleep may be used to issue alerts to caregivers to provide timely help to the patients. The contact-free nature of the PIR sensors and its ability to detect seizures even in the dark make them attractive for patient use. We note that while a sleep stage can trigger the epilepsy, which is noticeable in some epilepsy syndrome cases like Rolandic seizures, epilepsy may in turn disorganize and confuse sleep during epileptic seizures [25].

III. The Proposed System Design

A. Data Acquisition Using Passive Infrared PIR Sensor

PIR sensors are low-cost devices which can be used in affordable detection systems. They consume very little power and they can be efficiently used to detect body motion based on the infrared energy emitted by the human body. Unlike camera-based detection systems, invasion of privacy is not a concern with the use of PIR sensors. In contrast to visible-light devices, PIR sensors can also work in the dark [18], [21], [22]. A PIR sensor is made of two sensitive plates that can sense InfraRed (IR) radiation, and the output of the sensor is proportional to the difference in the IR radiation impinging on the two plates. When there is no motion, a zero output signal is generated because each plate detects the same amount of IR radiation. In contrast to that, a moving body causes a differential change in one plate when it moves in the sensing area. Most of the commercially available PIR sensors that are used for motion detection have a binary output. In this research, we use a sensing unit (SU) instead of a standalone PIR sensor. The SU consists of an array of Fresnel lenses, an IR filter, and a PIR sensing element which consists of three pins (GND, V_{cc} and binary output), analog circuitry, and a microcontroller (Arduino Nano) as shown in Figure 1.

Fresnel lenses are plano-convex lenses that permit the IR radiation to penetrate them. Basically, Fresnel lenses work

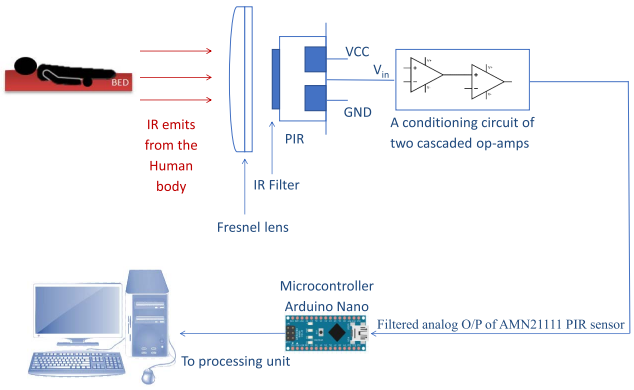

Fig. 1. Sensing unit (SU) in the proposed method that consists an array of Fresnel lenses, an IR filter, and PIR sensing elements.

as an antenna by increasing the range of captured IR and projecting it onto the sensing plates of the PIR sensor. Since the amplitude of the IR radiation decreases with distance, Fresnel lenses are also used to expand the range of the detecting distance for the PIR sensor.

The analog circuit of the SU is used to generate an analog output of the PIR sensor instead of the digital output. The maximum amplitude voltage of the PIR sensor is 3.3v and, therefore, voltage divider resistors are used to prevent any clipping in the amplitude of the analog output signal. The PIR signal is a low-amplitude signal and its frequency is less than 5 Hz [18], [20]. Epileptic seizures are characterized by rhythmic jerks of the body, and the average jerking rate in a seizure is about 2 jerks/second, and this can be captured in the signal acquired with a PIR sensor. Two operational amplifiers (op-amps), OA1 and OA2 (see Figure 2) are used as a cascaded stage in order to increase the amplitude of the PIR signal and bring it to a readable level. The two successive op-amps are also used to filter the signal from the unwanted noise. To filter noise from the signal, R_2, C_1 and R_5, C_4 at each stage act as a low pass filter with cut-off frequency equal to 1.6 Hz (see Equation 1 and 2). Because PIR sensors are intended to detect the human body motion with a frequency content less than 3 Hz, there is, therefore, no need to deal with high frequencies. R_4, C_3 and R_3, C_2 at each stage are used as a high pass filter to suppress the DC bias of the signal (see Equation 3 and 4).

$$f_{cutoff_1} = \frac{1}{2\pi R_2 C_1}, \tag{1}$$

$$f_{cutoff_2} = \frac{1}{2\pi R_5 C_4}, \tag{2}$$

$$f_{low_1} = \frac{1}{2\pi R_4 C_3}, \tag{3}$$

and

$$f_{low_2} = \frac{1}{2\pi R_3 C_2} \tag{4}$$

The gain for each stage is approximately equal to 100 (see Equation 5 and 6) which gives a total gain approximately equal to 10,000.

$$Gain_{OA1} = 1 + \frac{R_2}{R_4}, \tag{5}$$

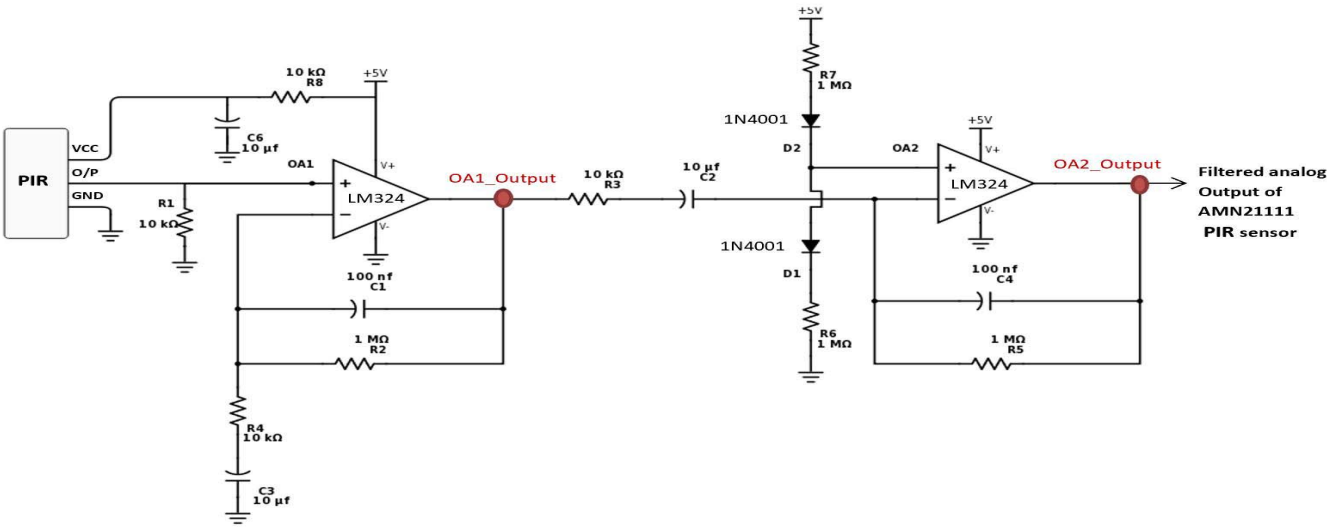

Fig. 2. A conditioning circuit of two cascaded op-amps to filter the analog input of the PIR sensor. The output of the second amplifier OA2_Output is the filtered analog output of the Panasonic AMN21111 PIR sensor.

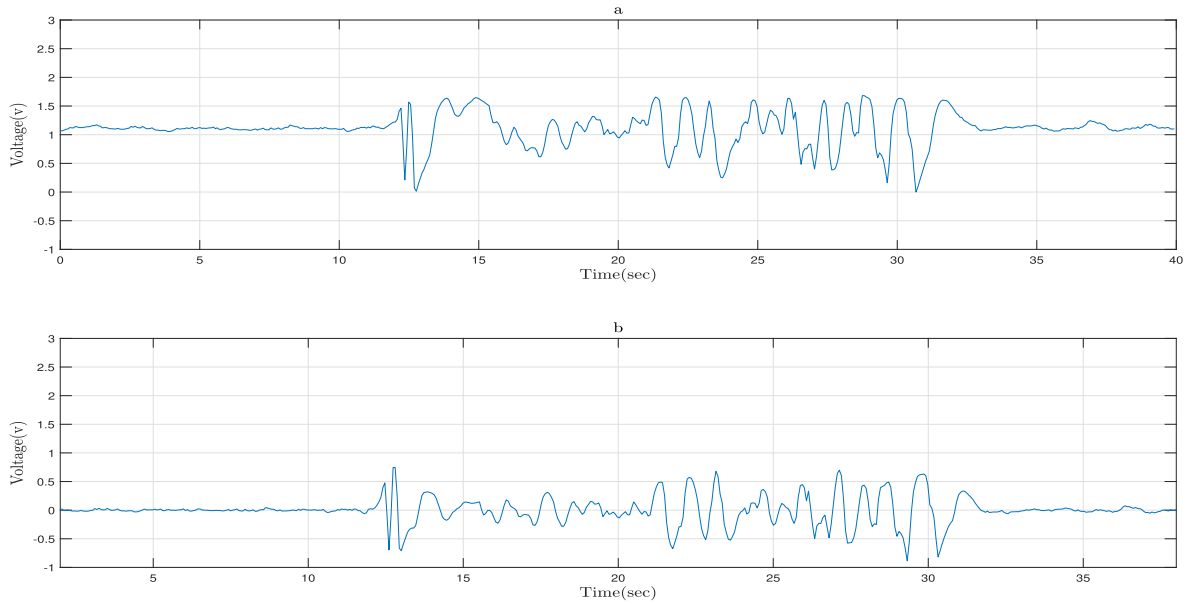

Fig. 3. a) PIR sensor signal corresponding to an epileptic seizure case, and b) its high-pass filtered version.

and

$$Gain_{OA2} = 1 + \frac{R_5}{R_3} \tag{6}$$

The output of OA2 is the filtered analog output signal of the PIR sensor. The filtered analog output is sampled and quantized with an Arduino nano microcontroller in order to be sent to the processing unit for classification. The sampling frequency used is 20 Hz with 10 bit quantization level.

The output signal of the PIR sensor contains a bias that can change with the room temperature. To remove this bias, the PIR sensor signal x[n] is convolved with a high-pass filter (HPF) with transfer function:

$$H(z) = h[0] + \sum_{n=1}^{10} h[n]\left(z^{-n} + z^{n}\right) \tag{7}$$

The high-pass filter is designed using a minimax magnitude criterion, with a normalized angular passband edge frequency of 0.1π and stopband edge frequency of 0.05π. Figure 4 shows a filtered PIR signal. The output $y[n]$ is obtained using convolution, $y[n] = x[n] * h[n]$.

IV. Feature Extraction and Classification

In order to design and build a precise model that can deal with a large amount of complex data and give accurate outcomes, many machine learning and deep learning algorithms are being used for the task of classification. In this study three different algorithms are used to extract features and classify the data captured from the PIR sensor, a) a Hidden Markov Model, b) a 1-D ConvNet, and c) a 2-D ConvNet and they are compared to each other.

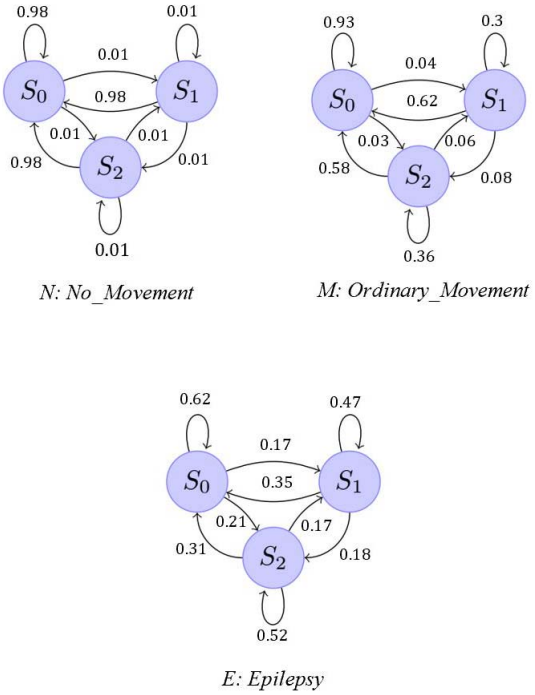

Fig. 4. Three HMM chains with three classes, no-movement (N), movement (M), and epileptic seizures (E).

A. Supervised Hidden Markov Model (HMM)

A supervised Hidden Markov Model is used to classify epileptic seizures and absence of epileptic seizures during a subject's sleep. In our study, we considered the normal movement during sleep and no movement during sleep as absence of epileptic seizure. Figure 3 shows three HMMs corresponding to three classes: Model E corresponds to the occurrence of epileptic seizures, model M corresponds to the normal movement of the subjects during sleep, and finally, model N corresponds to no-movement case during deep sleep.

We design three Markov models corresponding to epileptic seizures, normal movement during sleep, and no-movement during deep sleep from our training data [36]. The filtered PIR signal $y[n]$ is quantized into three levels using a threshold value of Th which is used to define the observation symbols, states and the corresponding transition probabilities for each model. This threshold value can be obtained by using a genetic algorithm based approach [24]. An estimated threshold $Th = 0.05\upsilon$ is used in our method. We have three states S_0, S_1 and S_2 and three observation symbols O_0, O_1 and O_2 in the three Markov models. The output $y[n]$ of the high-pass is quantized into three levels. The symbol O_0 represents the data when $y[n]$ is within the interval $[-Th, Th]$. O_1 represents the data when $y[n]$ is above the threshold Th, while O_2 represents the data when $y[n]$ is below $-Th$. In HMM framework, we cannot exactly know how the Baum-Welch training algorithm assigns the states [36]. Ideally, state S_0 may correspond to the case of $y[n]$ being in the interval $[-Th, Th]$. State S_1 may represent the data when $y[n]$ is above the threshold Th, while state S_2 may represent the data when $y[n]$ is below $-Th$. The states are hidden from us. Hence the designation Hidden Markov Model. We estimate the transition probabilities from our training data. Each model has different state transition probabilities estimated by the Baum-Welch training algorithm [36]. The probability of observing a sequence of symbols $O = \{o_1, \cdots, o_n\}$ given a state sequence $W = \{w_1, \cdots, w_n\}$ and the Markov model (No-Movement) is expressed as follows:

$$P(O \mid N) = \pi(w_1)P(o_1 \mid w_1)\prod_{t=2}^{n} P_r(t), \tag{8}$$

where

$$P_r(t) = A_{ij}B_{jk} = P(w_t \mid w_{t-1})P(o_t \mid w_t), \tag{9}$$

where π is the initial probability of starting with state w_1, n is the number of states in S, o_t represents the observed symbol at time t, A_{ij} is the state transition probability, $A_{ij} = p(w_t = S_j \mid w_{t-1} = S_i)$ and B_{jk} is probability of observing the k^{th} symbol o_k at the state $w_t = S_j$, $B_{jk} = P(o_k \mid w_t = S_j)$.

Similarly, we calculate

$$P(O \mid M) = \pi(w_1)P(o_1 \mid w_1)\prod_{t=2}^{n} P_r(t), \tag{10}$$

and

$$P(O \mid E) = \pi(w_1)P(o_1 \mid w_1)\prod_{t=2}^{n} P_r(t), \tag{11}$$

which represent the probabilities of movement and epilepsy classes, respectively. Finally, the classification decision is made based on the most probable class. Fast algorithms for computing the probabilities in (8), (10), and (11) are described in [36].

Each Markov model has different transition probability values because when there is no seizure the signal stays mostly within the threshold interval $[-Th, Th]$. Therefore, the model N has very high probability $p(S_0 \mid S_0)$ compared to other models. When there is an epileptic seizure, the signal oscillates between states frequently due to rhythmic jerks. Therefore, the state transition probabilities $p(S_i \mid S_j)$ $(i \neq j)$ of the model E is higher than those of the other models. In the "Ordinary_Movement" Markov model, the state transition probabilities of moving back to the resting state (S_0), $p(S_0 \mid S_1)$ and $p(S_0 \mid S_2)$, are higher than other state transition probabilities, because the subject goes back to static state after body movements or a turning up to the left or to the right.

B. 1-D ConvNet

Deep learning techniques are modeled to mimic the human brain ability to make an accurate decision for different complex problems [30]. A ConvNet is a discriminative deep learning model that is used to extract and classify features based on a combination of non-linear transformation operations and linear filters [30], [31]. The main building blocks of the 1-D ConvNet are convolution, activation function, and pooling [35]. The input to the 1-D ConvNet is a set of 396 time series vectors of PIR data collected from 33 subjects, as described below. The size of each vector is (1×764), where 764 represents the number of feature samples

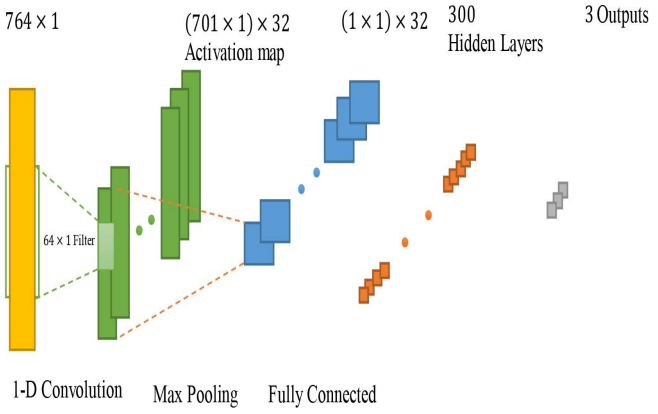

Fig. 5. The structure of 1D-ConvNet with max pooling layers, fully connected layer, and three outputs is used to classify the captured real-time series data using PIR sensor.

in each vector. The feature detector size is equal to (64 × 1) with a depth of 32 filters. To add a non-linearity to the ConvNet, an activation function must be applied after the convolution.

In this system, a Rectified Linear Unit (RELU) function is applied to the convolution layer. A max pooling or down sampling filter of size (1 × 701) (as shown in equation 12) is used to reduce the activation map dimensions, the network computations, and the number of parameters. The output of the max pooling layer, which represents the high-level extracted features of the input, is flattened and fed into a fully connected layer. A fully connected layer used in this system is a Neural Network (NN) of 300 hidden layers and three outputs. Finally, to prevent over-fitting, a dropout of 0.2 is applied to the output of the 1D-ConvNet. The softmax function is used to squash the output vector to ensure that the sum of the output probability is equal to one. Generally, the 1D-convolution and the max pooling layers are used to extract features from the input while the fully connected layer classifies the extracted features.

Figure 5 shows the 1D-ConvNet design that is used to classify the captured data signal via PIR. The size of activation map filter and the output of the max pooling layer depends on the size of the feature detector and the max pooling filter, the stride and the zero padding as shown in equation 12.

$$Filter\_Size = \left(\frac{W - F + 2P_d}{S_t}\right) + 1 \tag{12}$$

where W in this equation represents the height or width of the input image, F represents the size of the feature detector filter. P_d refers to the number of zeros padded and S_t is equal to the number of samples that the feature detector slides during the convolution operation.

C. 2-D ConvNet

The 2-D ConvNet layer consists of two convolutional layers, two max pooling layers and a fully connected layer. The data captured by the SU system are converted into spectrogram images, preprocessed, reshaped into (64×64) arrays with three input channels (RGB) and fed to the ConvNet. The input image matrices are convolved with a feature detector of size (3 × 3). An activation map of size (62 × 62 × 32) is produced. A down-sampling filter of size (2×2) is applied to reduce the size of the activation map. While there is loss of information due to down-sampling, the down-sampling or max pooling process reduces the number of calculations required for the next layers. The size of the filter after the first max pooling is (31×31×32), this filter is convolved with a feature detector of size (3 × 3) and down-sampled with a (2 × 2) filter before it flattened and fully connected to 128 hidden layers. The output of this network maps to one of three different classes. Figure 6 shows the structural layers of the proposed 2d ConvNet.

D. Captured Data Set

The sensor signal of our proposed SU system are sampled at 20 Hz frequency with 10-bit quantization. A total of 396 records (132 record for each class) are fed to the 1-D ConvNet. In order to measure the accuracy of our system and compare it with the activation accuracy of 1-D ConvNet, the data are mapped into spectrogram images and fed into a 2-D ConvNet. Figure 7 shows the signal corresponding to normal movements of the SU system. Figure 8 shows the PIR signal during epileptic seizure. For HMM, the observation data sets are partitioned into an observation data set for each class. The data set per each class are trained individually. The max loglikelihood of each test set data per class is computed to classify each observed window. Figure 9 shows the spectrogram images for the cases of no motion, normal movement, and epileptic seizure.

V. Evaluation Metric of the SU System

In many classification problems, one of the most important steps to get an optimum classifier is the selection of metrics. Confusion matrix is a measurement metric, it is an array of size n×n (true labels × predicted labels), where n is equal to the number of different classes [33]. For a binary classifier (n = 2), if the actual and predicted values are true, the class cell refers to true positive (TP). If both are false, then the class cell refers to true negative (TN). The confusion matrix gives a false positive (FP) when the actual value is false and predicted value is true. If the opposite happens, the class cell refers to false negative (FN). The related metric parameters can be represented mathematically as:

$$P_R = \frac{TP}{TP + FP}, \tag{13}$$

$$R_C = \frac{TP}{TP + FN}, \tag{14}$$

$$F1\_Score = 2 \times \frac{P_R \times R_C}{P_R + R_C}, \tag{15}$$

$$A_{CC} = \frac{TP + TN}{TP + FP + TN + FN}, \tag{16}$$

where P_R (Precision) is the ratio of correctly detected epileptic seizures to the total detected seizures, R_c (Recall or sensitivity) is the ratio of correctly detected epileptic seizures to all the class observations, $F1\_Score$ is harmonic mean of precision and sensitivity, and A_{cc} (Accuracy) is the probability of the model's correct predictions [33]. Since we have three

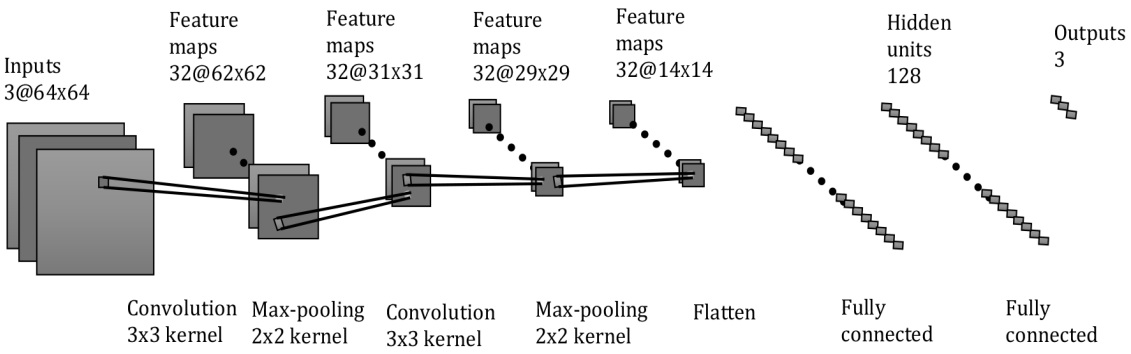

Fig. 6. 2D-ConvNet deep learning structure with two convolution layers and two max pooling layers that used to classify the spectogram images of the collected data.

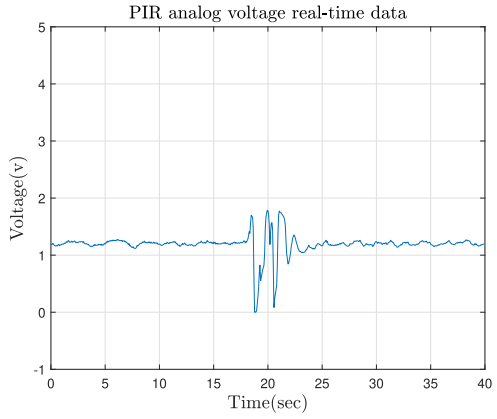

Fig. 7. The PIR signal due to normal movements selected from one of the 33 subjects, the session period is 40 second.

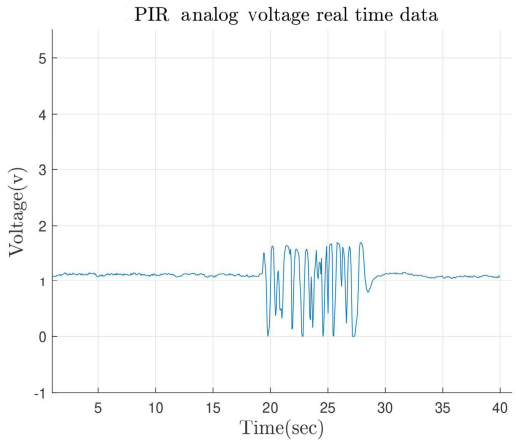

Fig. 8. The PIR signal due to epileptic seizure selected from one of the 33 subjects, the session period is 40 second.

classes in our work (Epileptic seizures, Normal-movement and No-movement), a confusion matrix of size 3×3 was used (see figure 10). The measurements of sensitivity and precision metrics for a certain class such as epileptic seizure class can be represented mathematically as follows:

$$Sensetivity_{Epilepsy} = \frac{C_{Epilepsy,Epilepsy}}{\sum_n T_{Epilepsy}}, \tag{17}$$

$$Precision_{Epilepsy} = \frac{C_{Epilepsy,Epilepsy}}{\sum_n P_{Epilepsy}}, \tag{18}$$

where $C_{Epilepsy,Epilepsy}$ is the confusion matrix element that represents the intersection of true label and predicted label of epileptic seizures class, $T_{Epilepsy}$ is the row elements of epileptic seizures class, $P_{Epilepsy}$ is the column elements of epileptic seizures class. The evaluation metrics for other classes are defined in a similar way [33].

VI. Results and Discussion

For this study we received an Institutional Review Board (IRB) approval to examine the use of our sensing method on healthy recruited subjects for the purpose of carrying out a preliminary study using data from simulated motions of seizure. This will enable us to establish an early proof of concept for epileptic seizure detection using PIR sensors. For access to patients experiencing real seizures, we are waiting for IRB approval in collaboration with physicians studying epilepsy patients. We recruited 27 male and 6 female healthy subjects for this study.

The subjects were asked to perform a set of activities following procedure that consists of 12 sessions of activities where each session lasts 40 seconds. Half of the sessions (6) are done in a lit room while the other half are done in a dark room.

Before the start of the procedure, the subjects were asked to watch a YouTube video of a patient experiencing a compulsive epileptic seizure. In each session, each subject was asked to lie down on a couch and perform a set of activities consisting of 1) pretending to sleep without moving; 2) mimicking motions of an epileptic seizure while pretending to be a sleep; 3) moving the body to change position during sleep to mimic normal occasional body movement. The data are collected through the SU system that we designed and transmitted to a dedicated PC. The PIR sensor is the central unit of the SU system and it works based on the IR energy received from the subject. There was no contact between the sensor and the subjects through the entire procedure.

To process and classify the captured data set, we initially examined the use of the signal frequency content for classification. Since the epileptic seizure class has the highest frequency content among the three classes (epileptic seizure, movement, and no movement), we computed the Discrete Fourier Transform (DFT) of the signal and defined features

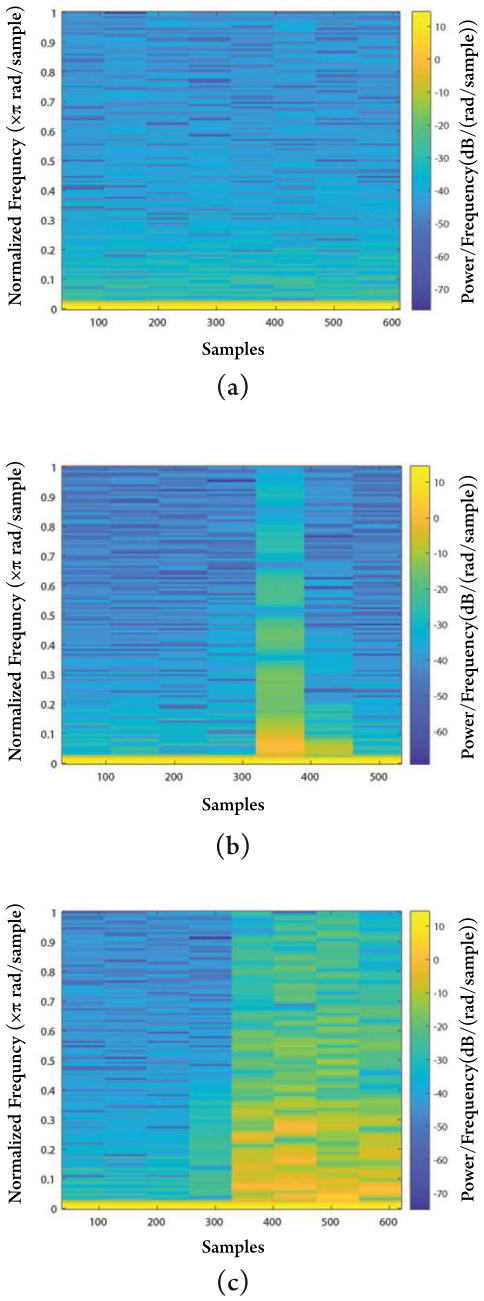

Fig. 9. Spectogram image of captured PIR signal for a) no motion, b) a normal movement, c) an Epliptic seizure, all the three images which selected randomly are belong to one of 33 subjects.

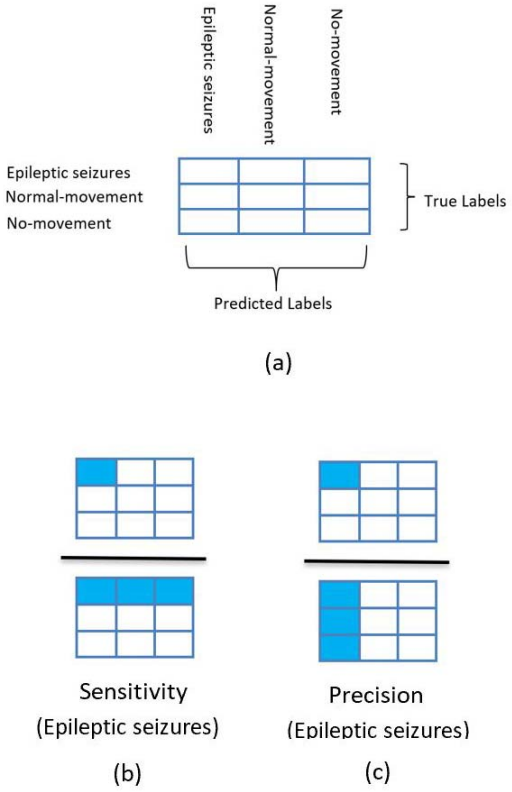

Fig. 10. (a) Confusion matrix, (b) sensitivity measurement of the epileptic seizures class, and (c) precision measurement of the epileptic seizures class.

TABLE I

THE STRUCTURAL LAYERS AND NUMBER OF PARAMETERS OF THE 1D CONVNET THAT GIVES THE TYPE OF LAYERS USED, THE SIZE OF EACH LAYER, AND THE NUMBER OF PARAMETERS EXTRACTED FROM EACH LAYER

Layer type	Output shape	parameters #
Conv 1d, 1 stride, 0 Padding	32 ×701 × 1	2080
RELU (Activation Function)	32 ×701 × 1	0
Max_poling, 1 stride, 0 Padding	32 ×1 × 1	0
Flatten_Hidden	32	0
Dense_Hidden	300	9900
Dropout (0.2)	300	0
Dense_Output	3	903
Softmax (Activation Function)	3	0

based on the fraction of the signal frequency content energy in suitably defined bands. We investigated features with different choices of frequency band boundaries and among these we chose the features that yielded the highest accuracy which was equal to 84.6%. The count of false positives was high, and we sought to improve the classification performance. Therefore, we examined the use of machine learning algorithms in order to enhance recognition accuracy.

A HMM algorithm was used to classify the collected data sets. As described before, three Markov models (epilepsy, ordinary movement and no-movement) were trained individually. The maximum log-likelihood of each test data set per class was measured to classify each suitable selected window of observation. The validation accuracy using HMM is 97.032%. In addition to that, two deep learning classification methods were used to classify the captured data. For the 1-D ConvNet, the data set are converted into 396 records. These records are split into 297 training records and 99 testing records (i.e. 75% training set and 25% test set). The data are fed into a multi-layer network that consists of a 1D Convolution layer, a flattening layer, and a fully connected layer (see Table I).

To prevent overfitting, a drop out of 0.2 and a softmax activation function are applied to the output [34]. All the epileptic seizure cases were correctly detected, and no false positive values appeared. On the other hand, 3 normal movement cases were misclassified as no-movement cases. Therefore, the validation accuracy of the system classification is equal to 96.97%, while the validation loss is equal to 0.06. Figure 11 shows

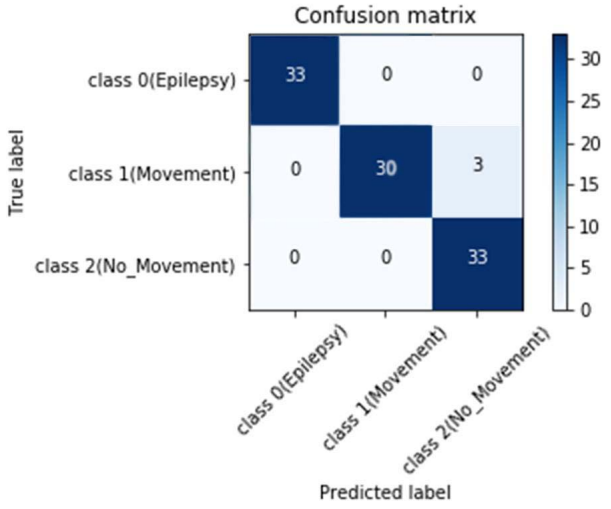

Fig. 11. A 3×3 two dimensional (true label vs predicted label) confusion matrix of 1D-ConvNet.

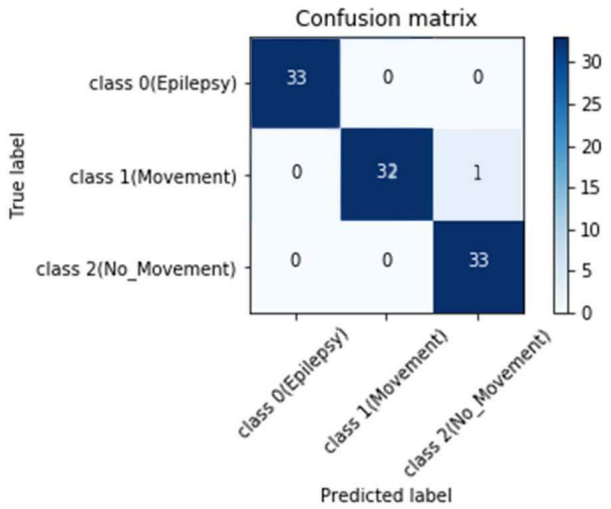

Fig. 12. A 3×3 two dimensional (true label vs predicted label) confusion matrix of 2D-ConvNet.

TABLE II

EVALUATION METRIC OF THE 1D CONVNET WHICH SHOWS THE VALUE OF PRECISION, AND RECALL, F1 SCORE FOR EACH OF THE THREE CLASSES: EPILEPTIC SEIZURE, NORMAL MOVEMENT, AND NO MOVEMENT

	Precision	Recall	F1-Score	Support
Class0(Epileptic Seizure)	1.00	1.00	1.00	33
Class1(Normal Movement)	1.00	0.91	0.95	33
Class2(No Movement)	0.92	1.00	0.96	33
Avg / total	0.97	0.97	0.97	99

TABLE III

THE STRUCTURAL LAYERS AND NUMBER OF PARAMETERS OF THE 2D CONVNET THAT GIVES THE TYPE OF LAYERS USED, THE SIZE OF EACH LAYER, AND THE NUMBER OF PARAMETERS EXTRACTED FROM EACH LAYER

Layer type	Output shape	no. of parameters
Conv 2d, 1 stride, 0 Pad	$32 \times 62 \times 62$	896
RELU (Activation Function)	$32 \times 62 \times 62$	0
Max$pooling2d, 2strides, 0Pad$	$32 \times 31 \times 31$	0
Conv 2d, 1 stride, 0 Padding	$32 \times 29 \times 29$	9248
RELU (Activation Function)	$32 \times 29 \times 29$	0
Max$pooling2d, 2strides, 0Pad$	$32 \times 14 \times 14$	0
Flatten	6272	0
Dense_Hidden	128	802944
Dense_Output	3	387
Softmax (Activation Function)	3	0

the confusion matrix of the designed network. 1D-ConvNet successfully detected all the seizures. The precision, recall and $F1\_Score$ evaluation metrics are also calculated (see Table II).

In the second method of data classification, the captured data was converted into spectrogram images. All the spectrogram images are reshaped into a (64×64) arrays and fed into a 2D ConvNet. The network designed consists of two convolutional layers with feature detector size (3×3) and depth 32 for each, two max pooling layers with down sampling filter of size 2×2 (2 stride and depth length 32) and a fully connected layer with 128 hidden layers and three outputs (see Table III). Excessive training causes the classifier to memorize the input data. In order to avoid the poor performance of the classifier, a K-fold cross validation is applied on the input data images to estimate the generalized performance of the classifier [23]. The set of images were divided into 12-fold groups of equal size (33 records). The first fold is used as a test dataset while the remaining folds are used as a training dataset. The accuracy and the other performance metrics are then calculated. The procedure was repeated twelve times. The total accuracy, precision, recall and $F1\_Score$ of this network are equal to the average of the K-fold cross validation trials (see Table IV). The validation accuracy of the 2D-ConvNet designed is equal to 98.98%. Figure 12 shows the confusion matrix of 2D-ConvNet design. Because of the use of the K-fold, all the spectrogram input images were used as a training set and as a data set during classification. It is observed in this study that the 2d_ConvNet gives better performance than the 1d_ConvNet, with higher accuracy and precision. However, in terms of speed HMM is the fastest machine learning algorithm (see Table IV, and Table V). The total number of parameters that are used in both networks depend on the size, the number of filters, the number of neurons that are used, and the way that they connect to the other neurons. This system is used to detect the generalized epileptic or generalized tonic-clonic seizure but not the partial seizure that happens in a certain part of the brain [25]. To use this system in patient monitoring, the sensor can be connected to a wireless network to alert a first response or a caregiver.

TABLE IV

EVALUATION METRIC OF THE 2D CONVNET WHICH SHOWS THE VALUE OF PRECISION, AND RECALL, F1 SCORE FOR EACH OF THE THREE CLASSES: EPILEPTIC SEIZURE, NORMAL MOVEMENT, AND NO MOVEMENT

	Precision	Recall	F1-Score	Support
Class0(Epileptic Seizure)	1.00	1.00	1.00	33
Class1(Normal Movement)	1.00	0.97	0.98	33
Class2(No Movement)	0.97	1.00	0.98	33
Avg / total	0.99	0.99	0.99	99

TABLE V

VALIDATION ACCURACY AND IMPLEMENTATION TIME OF EACH CLASSIFIER, HMM, 1D, AND 2D CONVNET

Classifier	Validation accuracy	Implementation time (μsec)
HMM	97.03%	00.02
1D_ConvNet	96.97%	07.10
2D_ConvNet	98.98%	92.20

TABLE VI

VALIDATION ACCURACY COMPARISON WITH OTHER MOTION SENSORS TO DETECT EPILEPTIC SEIZURES

Method	Type of sensor	Accuracy
Proposed	**PIR**	**98.98%**
Beniczky [4]	Wireless wrist accelerometer	89.00%
Nijsen [5]	3D-accelerometer	55.56%
Narechania [9]	mattress sensor	80.00%

VII. CONCLUSION

Our study shows that the system we devised can work as a real-time system and has the potential to be applied to subjects with epileptic seizures. We note that the results have been obtained for simulated seizures. We plan to perform the tests on patients with epilepsy after we receive IRB approval in collaboration with physicians studying epilepsy patients. Since all the seizures were detected successfully, the low-cost, low-power PIR sensor shows promise as a reliable device to detect epileptic seizures. Because of the contact-free nature of the PIR sensor, this can avoid discomfort with the use of such sensors during sleep. Furthermore, this system can work in the dark as well as with illumination. Additionally, the ambient light does not affect the sensitivity of the system. Finally, the cost of this system is lower than the other available monitoring cameras and sensors.

A variety of high-level machine learning and deep learning techniques were used to classify the captured signals from the PIR sensor. All the programs were implemented using a CPU E5-1620 V3, 3.5 GHz with 8 cores, Memory size 32 GB, and an operating system Centos 6.9. A comparison between the applied algorithms was done based on the validation accuracy, implementation time (See Table V), evaluation metric, confusion matrix, and structural design. We observe that the accuracy in Table V is equal to 97.03% for HMM, 96.97% for 1D_ConvNet, and 98.98% for 2D_ConvNet. We compared our results with the accuracy of the other motion-based epileptic seizure detection systems (see Table VI). We observe that our method shows significantly improved performance, while noting that it was achieved with data obtained from simulated epileptic seizures.

For real-time monitoring of a patient, the collected sensor data will be processed and classified using overlapping data segments. It is adequate to process and analyze the data segments at the rate of 15 to 20 times per minute. This provide 3-4 seconds of data acquisition and processing time to analyze the data. Given the processing times shown in Table V, it is clear that we can accomplish the processing and analysis within 3 seconds to support real-time monitoring. To improve the performance of the system we plan to investigate the use of an array of sensors.

REFERENCES

[1] H. Witte, L. D. Iasemidis, and B. Litt, "Special issue on epileptic seizure prediction," *IEEE Trans. Biomed. Eng.*, vol. 50, no. 5, pp. 537–539, May 2003.

[2] M. A. Kumar, S. Kishore, N. Karthik, K. C. Sekhar, M. C. Chinnaiah, and S. Shafi, "Realtime epileptic seizures detection and alert system using NI lab-view," *Int. J. Sci. Res. Publ.*, vol. 5, no. 5, pp. 478–482, 2014.

[3] J. Christensen, M. Vestergaard, M. G. Pedersen, C. B. Pedersen, J. Olsen, and P. Sidenius, "Incidence and prevalence of epilepsy in Denmark," *Epilepsy Res.*, vol. 76, no. 1, pp. 60–65, Aug. 2007.

[4] S. Beniczky, T. Polster, T. W. Kjaer, and H. Hjalgrim, "Detection of generalized tonic–clonic seizures by a wireless wrist accelerometer: A prospective, multicenter study," *Epilepsia*, vol. 54, no. 4, pp. e58–e61, Apr. 2013.

[5] T. M. E. Nijsen, J. B. A. M. Arends, P. A. M. Griep, and P. J. M. Cluitmans, "The potential value of three-dimensional accelerometry for detection of motor seizures in severe epilepsy," *Epilepsy Behav.*, vol. 7, no. 1, pp. 74–84, Aug. 2005.

[6] V. Strong, S. W. Brown, R. Walker, and S. Dogs, "Seizure-alert dogs—Fact or fiction?" *Seizure*, vol. 8, no. 1, pp. 62–65, 1999.

[7] V. Strong, S. Brown, M. Huyton, and H. Coyle, "Effect of trained seizure alert dogs on frequency of tonic–clonic seizures," *Seizure*, vol. 11, no. 6, pp. 402–405, Sep. 2002.

[8] Z. Li, A. M. D. Silva, and J. P. S. Cunha, "Movement quantification in epileptic seizures: A new approach to video-EEG analysis," *IEEE Trans. Biomed. Eng.*, vol. 49, no. 6, pp. 565–573, Jun. 2002.

[9] A. P. Narechania, I. I. Garić, I. Sen-Gupta, M. P. Macken, E. E. Gerard, and S. U. Schuele, "Assessment of a quasi-piezoelectric mattress monitor as a detection system for generalized convulsions," *Epilepsy Behav.*, vol. 28, no. 2, pp. 172–176, Aug. 2013.

[10] F. Pauri, F. Pierelli, G. E. Chatrian, and W. W. Erdly, "Long-term EEG-video-audio monitoring: Computer detection of focal EEG seizure patterns," *Electroencephalogr. Clin. Neurophysiol.*, vol. 82, no. 1, pp. 1–9, Jan. 1992.

[11] J. M. Rennie, G. Chorley, G. B. Boylan, R. Pressler, Y. Nguyen, and R. Hooper, "Non-expert use of the cerebral function monitor for neonatal seizure detection," *Arch. Disease Childhood-Fetal Neonatal Ed.*, vol. 89, no. 1, pp. F37–40, Jan. 2004.

[12] J. Gotman, "Automatic detection of seizures and spikes," *J. Clin. Neurophysiol.*, vol. 16, no. 2, pp. 130–140, Mar. 1999.

[13] J. Lockman, R. S. Fisher, and D. M. Olson, "Detection of seizure-like movements using a wrist accelerometer," *Epilepsy Behav.*, vol. 20, no. 4, pp. 638–641, Apr. 2011.

[14] R. Schuyler, A. White, K. Staley, and K. J. Cios, "Epileptic seizure detection," *IEEE Eng. Med. Biol. Mag.*, vol. 26, no. 2, pp. 74–82, Mar. 2007.

[15] A. T. Tzallas, M. G. Tsipouras, and D. I. Fotiadis, "Epileptic seizure detection in EEGs using time–frequency analysis," *IEEE Trans. Inf. Technol. Biomed.*, vol. 13, no. 5, pp. 703–710, Sep. 2009.

[16] J. Gotman, "Automatic seizure detection: Improvements and evaluation," *Electroencephalogr. Clin. Neurophysiol.*, vol. 76, no. 4, pp. 317–324, Oct. 1990.

[17] B. U. Toreyin, A. B. Soyer, I. Onaran, and E. E. Cetin, "Falling person detection using multi-sensor signal processing," *EURASIP J. Adv. Signal Process.*, vol. 2008, no. 1, Dec. 2007, Art. no. 149304.

[18] F. Erden *et al.*, "Wavelet based flickering flame detector using differential PIR sensors," *Fire Safety J.*, vol. 53, pp. 13–18, Oct. 2012.

[19] B. U. Töreyin, E. B. Soyer, O. Urfalioğlu, and A. E. Çetin, "Flame detection system based on wavelet analysis of PIR sensor signals with an HMM decision mechanism," in *Proc. 16th Eur. Signal Process. Conf. (EUSIPCO)*, Lausanne, Switzerland, Aug. 2008, pp. 1–5.

[20] F. Erden, E. B. Soyer, B. U. Toreyin, and A. E. Çetin, "VOC gas leak detection using Pyro-electric Infrared sensors," in *Proc. IEEE Int. Conf. Acoust., Speech Signal Process.*, Mar. 2010, pp. 1682–1685.

[21] F. Erden and A. E. Çetin, "Hand gesture based remote control system using infrared sensors and a camera," *IEEE Trans. Consum. Electron.*, vol. 60, no. 4, pp. 675–680, Nov. 2014.

[22] F. Erden, S. Velipasalar, A. E. Cetin, and A. Z. Alkar, "Sensors in assisted living: A survey of signal and image processing methods," *IEEE Signal Process. Mag.*, vol. 33, no. 2, pp. 36–44, Mar. 2016.

[23] Z. Zainuddin, L. K. Huong, and O. Pauline, "Reliable epileptic seizure detection using an improved wavelet neural network," *Australas. Med. J.*, vol. 6, no. 5, pp. 308–314, 2013.

[24] B. U. Töreyin, E. B. Soyer, O. Urfalıoğlu, and A. E. Çetin, "Flame detection system based on wavelet analysis of PIR sensor signals with an HMM decision mechanism," in *Proc. 16th Eur. Signal Process. Conf.*, 2008, pp. 1–5.
[25] R. Rocamora, J. C. Sánchez-Álvarez, and J. Salas-Puig, "The relationship between sleep and epilepsy," *Neurologist*, vol. 14, no. 6, pp. S35–S43, Nov. 2008.
[26] D. Minecan, A. Natarajan, M. Marzec, and B. Malow, "Relationship of epileptic seizures to sleep stage and sleep depth," *Sleep*, vol. 25, no. 8, pp. 899–904, Dec. 2002.
[27] M. H. Kryger, T. Roth, and W. C. Dement, *Principles and Practice of Sleep Medicine*. Amsterdam, Netherlands: Elsevier, 2005.
[28] C. Iber, S. Ancoli-Israel, A.-L. Chesson, and S. F. Quan, "The AASM Manual for the scoring of sleep and related events: Rules, terminology and technical specifications," 1st ed. Westchester, IL, USA: Amer. Acad. Sleep Med., Tech. Rep. Library of Congress Control Number: 0-9657220-4-X, 2007.
[29] M. G. Terzano, L. Parrino, S. Anelli, M. Boselli, and B. Clemens, "Effects of generalized interictal EEG discharges on sleep stability: Assessment by means of cyclic alternating pattern," *Epilepsia*, vol. 33, no. 2, pp. 317–326, Mar. 1992.
[30] L. Deng and D. Yu, "Deep learning: Methods and applications," *Found. Trends Signal Process.*, vol. 7, nos. 3–4, pp. 197–387, Jun. 2014.
[31] Y. Bengio, "Learning deep architectures for AI," *Found. Trends Mach. Learn.*, vol. 2, no. 1, pp. 1–127, 2009.
[32] S. Visa, B. Ramsay, A. Ralescu, and E. Van Der Knaap, "Confusion matrix-based feature selection," in *Proc. Midwest Artif. Intell. Cognitive Sci. Conf.*, Jan. 2011, pp. 120–127.
[33] C. Beleites, R. Salzer, and V. Sergo, "Validation of soft classification models using partial class memberships: An extended concept of sensitivity & co. Applied to grading of astrocytoma tissues," *Chemometrics Intell. Lab. Syst.*, vol. 122, pp. 12–22, Jan. 2013.
[34] N. Srivastava, G. Hinton, A. Krizhevsky, and R. Salakhutdinov, "Dropout: A Simple Way to Prevent Neural Networks from Overfitting," *J. Mach. Learn. Res.*, vol. 15, no. 1, pp. 1929–1958, 2014.
[35] Y. LeCun, L. Bottou, Y. Bengio, and P. Haffner, "Gradient-based learning applied to document recognition," *Proc. IEEE*, vol. 86, no. 11, pp. 2278–2324, Nov. 1998.
[36] L. Rabiner, "A tutorial on hidden Markov models and selected applications in speech recognition," *Proc. IEEE*, vol. 77, no. 2, pp. 257–286, Feb. 1989.
[37] H. Kapu, K. Saraswat, Y. Ozturk, and A. E. Cetin, "Resting heart rate estimation using PIR sensors," *Infr. Phys. Technol.*, vol. 85, pp. 56–61, Sep. 2017.
[38] F. Erden and A. E. Cetin, "Period estimation of an almost periodic signal using persistent homology with application to respiratory rate measurement," *IEEE Signal Process. Lett.*, vol. 24, no. 7, pp. 958–962, Jul. 2017.
[39] D. Zhi, "Depth camera-based hand gesture recognition for training a robot to perform sign language," M.S. thesis, Fac. Eng., School Elect. Eng. Comput. Sci., Ottawa-Carleton Inst. Comput. Sci., Univ. Ottawa, Ottawa, ON, Canada, 2018.
[40] *Data Sheet of AMN Series Panasonic PIR Sensors*. Accessed: Jan. 2017. [Online]. Available: https://www.components-mart.fr/datasheets/dc/AMN23112.pdf

Ouday Hanosh received the B.S. and M.S. degrees in electrical engineering from the College of Engineering, University of Baghdad, Baghdad, Iraq, in 1996 and 2001, respectively. He is currently pursuing the Ph.D. degree with the Department of Electrical and Computer Engineering, University of Illinois at Chicago. His research interests are signal processing, motion-based sensors, machine learning, and deep learning.

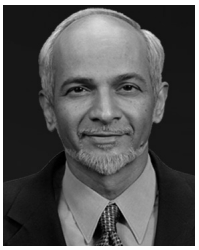

Rashid Ansari (F'99) received the B.Tech. and M.Tech. degrees in electrical engineering from the Indian Institute of Technology, Kanpur, India, and the Ph.D. degree in electrical engineering and computer science from Princeton University, Princeton, NJ, USA, in 1981. He served as a Research Scientist with Bell Communications Research and on the Faculty of Electrical Engineering, University of Pennsylvania. He is currently a Professor and the Head of the Department of Electrical and Computer Engineering, University of Illinois at Chicago (UIC). His research interests are in the general areas of signal processing and communications, with recent focus on image and video analysis, multimedia communication, and medical imaging.

Dr. Ansari was a member of the Editorial Board of the *Journal of Visual Communication and Image Representation*. He has served as a member of the Digital Signal Processing Technical Committee of the IEEE Circuits and Systems Society and the Image, Video, and Multidimensional Signal Processing Technical Committee. He was a member of the organizing and program committees of several past IEEE conferences. He served on the organizing and executive committees of the Visual Communication and Image Processing (VCIP) Conferences and was the General Chair of the 1996 VCIP Conference. He served as an Associate Editor for the IEEE TRANSACTIONS ON IMAGE PROCESSING, the IEEE SIGNAL PROCESSING LETTERS, and the IEEE TRANSACTIONS ON CIRCUITS AND SYSTEMS.

Khaled Younis received the B.Sc. degree from Mutah University, Jordan, and the Ph.D. degree in computer engineering from the University of Dayton, OH, USA. He was on the faculty of The University of Jordan from 2006 to 2008 and from 2015 to 2018. He was a Visiting Assistant Professor with the University of Chicago at Illinois, USA, in 2017, when he started working on this paper. He is on leave from The University of Jordan. He is currently a Staff Data Scientist with GE Healthcare working on applying artificial intelligence in X-ray. He has over 20 years of experience in medical imaging with extensive industry engagement working for iCAD, Inc. and TeraRecon, Inc. He has published numerous research papers in international journals, conference proceedings, and book chapters. His research interests are in machine learning, computer vision, and healthcare applications.

A. Enis Cetin (F'10) received the B.Sc. degree from METU, Ankara, Turkey, and the Ph.D. degree from the University of Pennsylvania in 1987. He was an Assistant Professor with the University of Toronto from 1987 to 1989. He was on the faculty of Bilkent University, Ankara, Turkey, from 1989 to 2016. He is on leave from Bilkent University. He is currently a Research Professor with the University of Illinois at Chicago. He has coauthored the book *Methods and Techniques for Fire Detection: Signal, Image and Video Processing Perspectives* (Academic Press; 2016) and the paper "Flame Detection for Video-Based Early Fire Warning for the Protection of Cultural Heritage," which received the Best Paper Award in a conference organized by the European Union and UNESCO. His research interests include signal, data, image, and video processing. He is the Editor-in-Chief of *Signal, Image and Video Processing* (Springer).